Flame Heights in Wall Fires: Effects of Width, Confinement and Pyrolysis Length

COUTIN M. and MOST J.M.
Laboratoire de Combustion et de Détonique
UPR 9028 au CNRS - ENSMA
86960 Futuroscope Cedex, FRANCE

DELICHATSIOS M.A.
Fire Science and Technology Laboratory
CSIRO - Div of Building Construction & Engineering
PO Box 310, North Ryde NSW 1670, AUSTRALIA

DELICHATSIOS M.M.
TEXTRON Systems
Boston, Massachusetts, USA

ABSTRACT

A new, consistent and objective methodology, using a CCD camera to map flame luminosity, was applied for measuring wall flame heights. Experiments in six distinct wall configurations were conducted by simulating a wall fire via gaseous burners. The wall width was fixed at 0.4m and the burner height was set at 0.25m, at 0.5m, or at 1m. In a first time, the wall, 2m high, was confined by water cooled (65° C) sidewalls a) over its total height so that the flames were entraining air from the front only or b) over its lower part beyond which flames were unconfined and could also entrain air sidewise. Then, the wall was unconfined over its total height (2.5m high) and the air was entrained from the front and at the side. Three fuels were tested : methane, propane and acetylene. The present consistent and objective wall flame height measurements were essential for the development of new wall flame height correlations that include effects of burner (pyrolysis) height, wall width and confinement by sidewalls.

KEYWORDS : wall fire, flame height correlations, gaseous burner, pyrolysis length, confined diffusion flame.

INTRODUCTION

Flame height in fires is a parameter needed to predict heat fluxes and release and dispersion of products of combustion. A common method for defining flame heights is based on visual observations [1]. Other methods include average temperatures on the fire axis [2], or radiative heat flux (or radiance) distribution along the fire axis [3]. The flame height corresponds to the end of burning owing to fuel consumption and all cited methods provide just a measure of the extent of burning.

In the present work a CCD camera (768x574 resolution and 8-bit grayscale) was used to measure and map the flame luminosity [4, 5]. A threshold value of luminous intensity identified the flame location in the instantaneous images [4, 5]. Three methods were applied to determine flame heights :

1. All intensities in the instantaneous images (160 total) were averaged to obtain an average image of the flame luminosity. The visible flame height is obtained by selecting an appropriate threshold.
2. A binary identification for flame location was applied on each instantaneous image by assigning zero (0) to a point having intensity less than a threshold value and one (1) otherwise. This threshold defines the flame location. Subsequently, the binary notations were averaged.
3. The instantaneous images were statistically treated using Zukoski's [6] criterion to determine flame heights when flame intermittency on the axis was 50%.

The luminosity threshold was selected to define the visible flame edge [4, 5]. It was also checked that the so-determined flame height corresponds to an average gas temperature of 500°C on the axis [4, 5]. All three methods yield nearly the same values.

EXPERIMENTAL SETUP

Six configurations were tested in the present program :

1. In the first configuration (Fig. 1a) a gaseous burner 0.50m high and 0.40m wide produced the wall flames. Water cooled sidewalls (65°C) restricted side entrainment over a height H=2m from the bottom of the burner.
2. In the second configuration (Fig. 1b), a gaseous burner 0.25m high and 0.40m wide was used. Water cooled sidewalls (65°C) restricted side entrainment over a height H=2m from the bottom of the burner.
3. In the third configuration (Fig. 2a), the same burner as in Fig. 1a was tested having sidewalls over a height of H=1m from the burner bottom. Sidewalls were not installed downstream of this height.
4. In the fourth configuration (Fig. 2b), the same burner as in Fig. 1b was tested having sidewalls over a height of H=0.75m from the burner bottom. Sidewalls were not installed downstream of this height.
5. In the fifth configuration (Fig. 3a), a gaseous burner 1m high was tested. Two water cooled sidewalls were placed each other sides of the wall, then side entrainment air was not restricted. A tube with a line of holes stabilized the diffusion flame at the bottom of the burner.
6. In the sixth configuration (Fig. 3b), the same burner as in first configuration was used (H=0).

For configurations 1, 2, 5 and 6 propane was tested whereas for configurations 3 and 4 methane, propane and acetylene were used. Zero point of the flames correspond to the bottom of the porous burner. Flame heights are listed in tables (Figs 1, 2 and 3) where four flame heights are shown for

each test obtained as described earlier :

1. L_{int} (m) from average luminous image fields [4, 5].
2. L_{bin} (m) from binary identification of flame on each instantaneous image and then, by averaging [4, 5].
3. L_{fluc} (m) from the 50% intermittency criterion.
4. L_f (m) is an average of the three previous measurements.

It is an indication of the "goodness" of the present flame height determination that all three measuring methods provide almost the same values.
Analysis and correlations of the results in tables follows next.

ANALYSIS AND CORRELATIONS

Entirely Confined Flows, Configurations 1 and 2 (Fig 1)

In these cases, it is expected that the wall width will not affect the flame heights because entrainment occurs from the front. The flame heights should correlate as [7, 8, 9] :

$$\frac{L_f}{\dot{Q}^{*\prime 2/3}} = \text{function}\left(\frac{\dot{Q}^{*\prime 2/3}}{L_b}\right) \tag{1a}$$

$$\text{or equivalently : } \frac{L_f}{L_b} = \text{function}\left(\frac{\dot{Q}^{*\prime 2/3}}{L_b}\right) \tag{1b}$$

where L_f is the flame height and L_b is the burner height (equal to 0.5m for configuration 1 and 0.25m for configuration 2). In addition, $\dot{Q}^{*\prime}$ is a dimensionless fire Froude number for wall fires [6,7,8] having the following simplified form :

$$\dot{Q}^{*\prime} = \frac{\dot{Q}'_{th}}{\rho_\infty C_{p\infty} T_\infty \sqrt{g}} \tag{1c}$$

where $\dot{Q}'_{th}$ is the theoretical heat release $\dot{Q}_{th}$ divided by the burner width l_b (= 0.4m for all tests).

Note that a more appropriate form for Eq. 1c would have been if the theoretical heat release rate would have been replaced by $\dot{Q}'_{ch} = \chi_A \dot{Q}'_{th}$, where χ_A is the combustion efficiency.

In deriving Eq. 1b, we have used the following physics [7, 8, 9] :

1. The flame height is determined by the turbulent flow in the outer part of the wall boundary layer and not by the viscous layer at the wall.
2. Turbulent mixing in the boundary layer controls combustion.
3. For modeling purposes, visible height is defined as the location where the mean concentration of fuel and its decomposition products is zero. This location will depend on the stoichiometric ratio and the level of fluctuations [8, 9]. It can be shown that this location on the axis occurs when the

entrainment of air to this location is a multiple of the air stoichiometric requirements for complete combustion. This multiplying factor depends on the level of fluctuations [8, 9].

Under these conditions, there is a length scale that characterizes the flame extent (length or width) which is proportional to [7, 8, 9] :

$$\text{combustion length scale} = \text{function}(\dot{Q}^{*\prime 2/3})$$

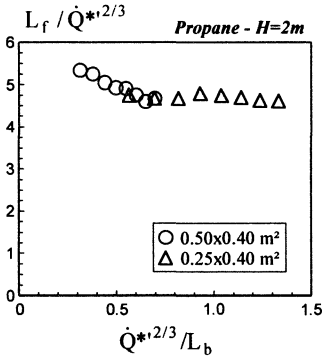

Figure 4a

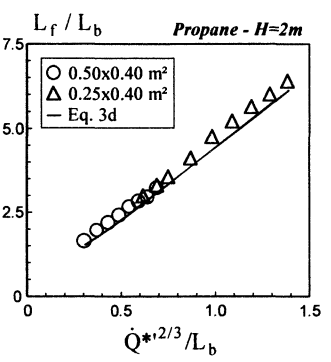

Figure 4b

Figure 4: Effects of burner height (pyrolysis length) on wall flame height in configurations having water cooled sidewalls (see Figs. 1a and 1b).

Data for propane wall flame heights are plotted in Figs 4a and 4b by using the suggested correlations by Eqs 1a and 1b respectively. It is seen from Figs 4a and 4b that the burner height (which can be identified as the pyrolysis height) only affects the flame height relation at small flame heights when the dimensionless numbers are :

$$\frac{\dot{Q}^{*\prime 2/3}}{L_b} \leq 0.4, \quad \frac{L_f}{L_b} \leq 2$$

This effect has been observed in previous work [8, 9]. For greater values of these parameters, the flame height for propane is given by :

$$L_f = 4.4\dot{Q}^{*\prime 2/3} \tag{2}$$

which agrees with previous correlations [7, 8, 9].

We can find a limiting correlation for $L_f / L_b \leq 2$ by noting that in this case [8, 9] combustion near the surface is characterized by a different length scale which depends only on the heat release rate

per unit surface area. This length scale behaves as :

$$L_m \approx \left(\frac{\dot{Q}'_{th}}{L_b} \right)^2 \tag{3a}$$

where we have left out parameters (such as gas properties and gravitational acceleration) which would make this relation dimensionally consistent (see Ref. 9 for details).
Flame heights in this regime would be dependent only on this length scale as :

$$L_f - L_b \approx L_m \approx \left(\frac{\dot{Q}'_{th}}{L_b} \right)^2 \tag{3b}$$

This result is consistent with the present experimental data shown in Figs. 4a and 4b. Eq. 3b is expressed in terms of the previous parameters as :

$$\frac{L_f - L_b}{L_b} \approx \left(\frac{\dot{Q}^{*\prime 2/3}}{L_b} \right)^3 \tag{3c}$$

Combining this with Eq. 2 and using the experimental data in Figs. 4a and 4b, we obtain a correlation valid in the whole range of parameters :

$$\frac{L_f}{L_b} = \left[1 + 85.2 \left(\frac{\dot{Q}^{*\prime 2/3}}{L_b} \right)^3 \right]^{1/3} \tag{3d}$$

namely, a relation that has appropriate limits and compares well with experiments as shown in Fig. 4b.

Partially Confined Flows, Configurations 3 and 4 (Fig 2)

For most of these results (Tables 2a and 2b) flame heights are larger than the confinement height H, which is 1m in Fig. 2a and 0.75m in Fig. 2b. Limiting our attention primarily to these data, we can be sure that the burner height should not enter in a proposed correlation, because $L_f / L_b \geq 2$ (cf. discussion in the previous section). We can, therefore propose the following correlation for flame heights :

$$\frac{L_f}{\dot{Q}^{*\prime 2/3}} = \text{function} \left(\frac{\dot{Q}^{*\prime 2/3}}{H}, \frac{\dot{Q}^{*\prime 2/3}}{l_b} \right) \tag{4a}$$

$$\text{or in a reduced form : } \frac{L_f}{\dot{Q}^{*\prime 2/3}} = \text{function} \left(\frac{L_f - H}{l_b} \right) \tag{4b}$$

In the second form, we have combined the two effects shown in Eq. 4a, namely the effects of confinement height H and wall width l_b which is equal to 0.4m for all tests.

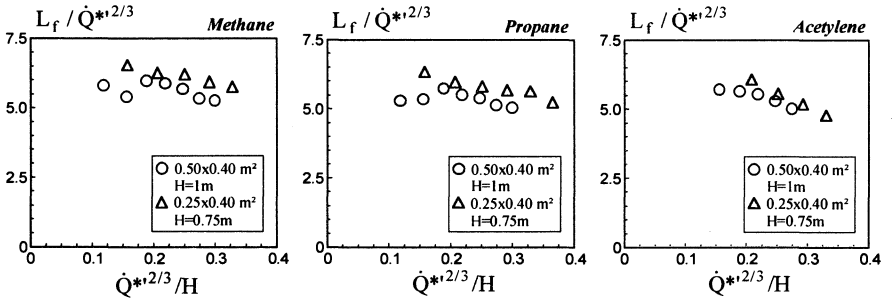

Figure 5a : Effects of partial confinement on wall flame heights. Coordinates correspond to correlation in Eq. 4a (Configurations 3 and 4 - three fuels).

These correlations have been used to plot the experimental flame heights listed in Tables 2a and 2b for three fuels and configurations 3 and 4. Figures 5a and 5b use coordinates corresponding to Eqs. 4a and 4b, respectively. Both correlations collapse the data well. The correlation in Fig. 5a plots the normalized height in terms of $\dot{Q}^{*1/3}/H$ indicating that the other parameter on the right hand side of Eq. 4a is not as important. We think that this reflects only the range of parameters of the present data.

We prefer the correlation in Fig. 5b (which also combines in one the two parameters on the right hand side of Eq. 4a), because its form is intuitively more physical and also because it collapses the data better than the correlation in Fig. 5a does.

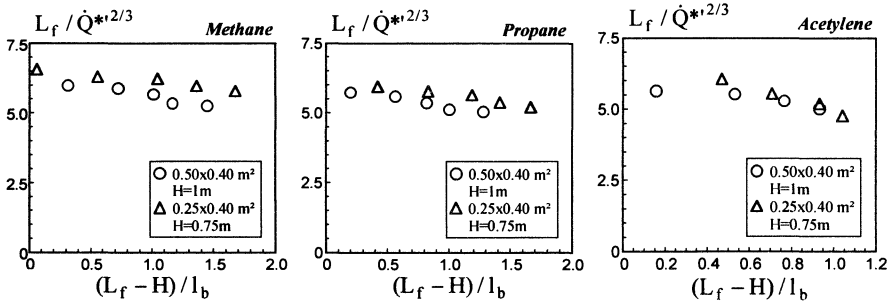

Figure 5b : Same that Fig. 5a except that coordinates suggested by Eq. 4b were used (Configurations 3 and 4 - three fuels).

The following remarks show the importance and limitations of proposed correlations :

1. All data are included in Fig. 5a, including data for which the flame height is less than the confinement height, $L_f \leq H$. By contrast, only the data for which $L_f \geq H$ are included in Fig. 5b.

2. Note in Fig. 5a that the first two normalized flame heights, where $L_f \leq H$, for configuration 3 (H=1m, Fig. 2a), are significantly smaller than the normalized heights when $L_f \geq H$ for all fuels. This result is contrary to expectations which would predict a smaller normalized height owing to larger entrainment (from the sides) as soon as sidewalls are absent, namely when $L_f \geq H$. We think, as other evidence also suggests [4, 5], that this behavior is due to increased fluctuations when sidewalls are not present. Increased fluctuations can decrease local combustion intensities and hence, would make flame heights larger even if entrainment increases. Also note that in the tests having sidewalls over the flame extent (see Figs. 4a and 4b), the (asymptotic) normalized flame height (for propane, Eq. 2) has a lower value than in the tests included in Figs 5a and 5b for propane.

The following correlations have been found by fitting the data in Fig. 5b:

METHANE

$$\frac{L_f}{\dot{Q}^{*2/3}} = \frac{6.5}{1 + 0.122\,\frac{L_f - H}{l_b}} \tag{5a}$$

PROPANE

$$\frac{L_f}{\dot{Q}^{*2/3}} = \frac{6}{1 + 0.122\,\frac{L_f - H}{l_b}} \tag{5b}$$

ACETYLENE

$$\frac{L_f}{\dot{Q}^{*2/3}} = \frac{5.7}{1 + 0.122\,\frac{L_f - H}{l_b}} \tag{5c}$$

These correlations are applicable for the following conditions :

$$\frac{L_f}{L_b} \geq 1.5 \tag{6a}$$

$$0 \leq \frac{L_f - H}{l_b} \leq 2 \tag{6b}$$

and of course $H \geq 0$.

The difference in the numerators of Eqs. 5a, 5b and 5c for the three different fuels is due to the different efficiency combustion for the three fuels: χ_A=1 for methane, χ_A=0.9 for propane and χ_A=0.78 for acetylene [10] see discussion page 3.

Unconfined Flows, Configurations 5 and 6 (Fig. 3)

The range of parameters as shown in Eqs 6a and 6b is extended, the last one being of more interest. We do expect the following behavior as this parameter defined by Eq. 6b increases (for H=0) :

$$\frac{L_f}{\dot{Q}^{*1/3}} = \text{function}\left(\left(\frac{L_f}{l_b}\right)^{-2/3}\right) \tag{7a}$$

which implies that the flame height varies as : $L_f = \text{function}(\dot{Q}_{th}^{2/5})$ (7b)
i.e. it is independent of wall width , l_b.

Using the suggested correlation by Eq. 7a, data for unconfined wall flame heights is plotted in Fig 6a. As for entirely confined flows, it is seen that the burner height affects the flame height relation when $L_f / L_b < \text{cte}$ (cte = 1.5) .
For greater values of this parameter, the following correlations collapse the data well (respectively Figs. 6b and 6c) :

$$\frac{L_f}{\dot{Q}^{*1/3}} = \frac{6.5}{1 + \left(\frac{L_f}{l_b}\right)^{-2/3} - 0.31} \tag{8a}$$

$$L_f = 0.40\dot{Q}_{th}^{2/5} - 0.49 \tag{8b}$$

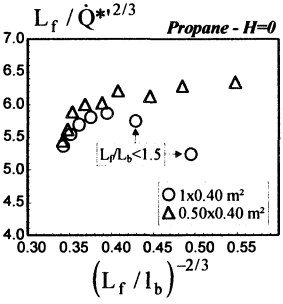

Figure 6a

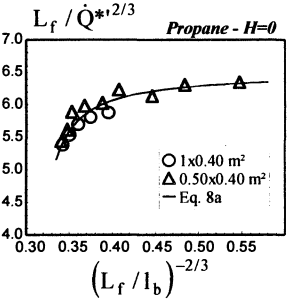

Figure 6b

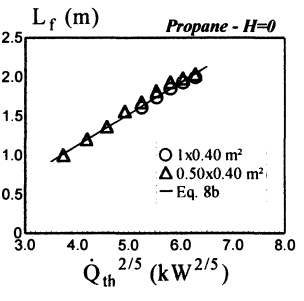

Figure 6c

Figure 6 : Effects of no confinement on wall flame heights.

Following the transition from confined (sidewalls) to unconfined (no sidewall) conditions, the normalized flame height decreases, as expected, because entrainment increases from the sides, whereas fluctuations remain the same in this regime.

CONCLUSIONS

A new, consistent and objective methodology [4, 5] using a CCD camera to map flame luminosity, was applied for measuring flame heights in wall fires.

The main results are :

1. Effects of pyrolysis length (here height of burner) on flame height, L_b, have been established (Figs. 4a and 4b) and a new correlation (Eq. 3d) has been developed which extends flame height correlations for cases where the flame height is comparable to pyrolysis height ($L_f \sim L_b$). This is an important situation for obtaining critical conditions for flame spread [9].
2. Effects of sidewall confinement and width have been investigated for three fuels and important correlations were developed (Eqs. 5a, 5b, 5c), admittedly, for a limited range of relevant parameters (Eqs. 6a, 6b).
3. By comparing measured flame heights, there is an indication that normalized flame heights ($L_f/Q^{*2/3}$) in confined (sidewall) situations are smaller than normalized flame heights in unconfined (no sidewall) situations (contrary to intuition) despite the larger entrainment rates in the latter case in comparison to the former case (cf. Eqs. 2, 5b and 8a). This behavior has also been observed in other experiments for pool type fires [4, 5]. We have proposed that this behavior is due to larger fluctuations in an "unconfined" situation, which would lead to a decrease of local burning intensities and hence, larger flame heights needed to complete combustion, even though entrainment might increase.

AKNOWLEDGMENTS

The experiments in this study were partially supported by the European Community Commission in the Framework of the ENVIRONMENT program for the environment (DG XII) with the Financial support of the « Institut de Protection et de Sureté Nucléaire » through the « Laboratoire d' Experimentation et de Modelisation des Feux (Jean-Claude Malet) », coordinator of the MISTRAL 1 and 2 projects.

REFERENCES

[1] Steward, F.R., Combustion Science and Technology, vol. 2, pp. 203-212, 1970.
[2] Heskestad, G., Fire Safety Journal, n°5, pp. 103-108, 1983.
[3] Ahmad, T. and Faeth, G.M., Seventeenth Symposium (International) on Combustion, The Combustion Institute, pp. 1149-1160, 1979.
[4] Audoin, L., Ph. D. Thesis, Université de Poitiers, France, January 24, 1995, see also Fire Safety Journal, n°24, pp. 167-187, 1995.
[5] Kolb, G., Ph. D. Thesis, Université de Poitiers, France, March 22, 1996.
[6] Zukoski, E.E., Kubota, T. and Cetegen, B.M., Fire Safety Journal, n°3, pp. 107-121, 1981.
[7] Delichatsios, M.A., Combustion Science and Technology, vol. 39, pp. 195-214, 1984.
[8] Delichatsios, M.A., Combustion and Flame, vol. 70, 33-46, 1987.
[9] Delichatsios, M.A., Combustion Science and Technology, vol. 106, pp. 125-136, 1995.
[10] Tewarson, A., FMRC Report J.I.0R0J4.RC (3), 1995.

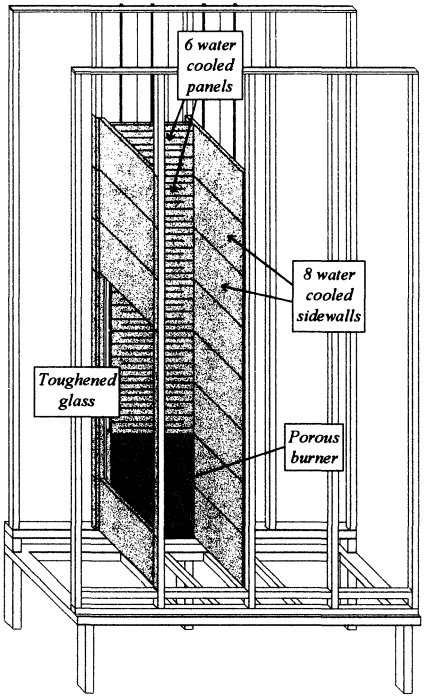

Figure 1a
Burner of 0.50x0.40 m²

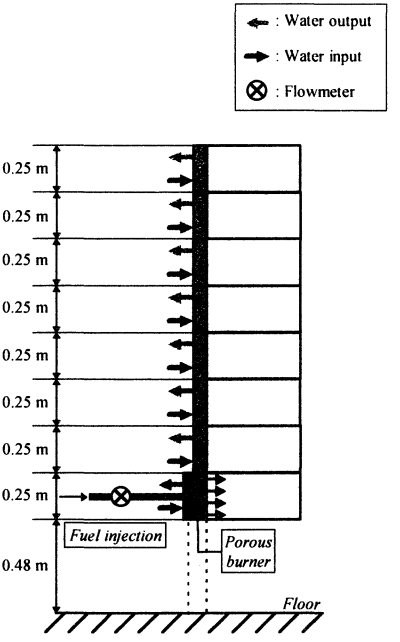

Figure 1b
Burner of 0.25x0.40 m²

	Q_{th} (kW)	L_{int} (m)	L_{bin} (m)	L_{fluc} (m)	L_f (m)
C_3H_8	**27**	0.834	0.827	0.827	**0.829**
	36	0.988	0.977	0.999	**0.988**
	45	1.102	1.092	1.109	**1.103**
	54	1.212	1.219	1.211	**1.214**
	63	1.341	1.337	1.342	**1.340**
	72	1.412	1.423	1.421	**1.419**
	81	1.483	1.487	1.490	**1.487**
	90	1.619	1.619	1.619	**1.619**

Table 1a
Burner of 0.50x0.40 m²

	Q_{th} (kW)	L_{int} (m)	L_{bin} (m)	L_{fluc} (m)	L_f (m)
C_3H_8	**27**	0.737	0.733	0.723	**0.731**
	36	0.875	0.868	0.872	**0.872**
	45	1.006	1.010	1.023	**1.013**
	54	1.166	1.166	1.182	**1.171**
	63	1.276	1.283	1.297	**1.285**
	72	1.397	1.386	1.390	**1.391**
	81	1.485	1.489	1.480	**1.485**
	90	1.581	1.577	1.590	**1.583**

Table 1b
Burner of 0.25x0.40 m²

FIGURE 1 : Experimental setup and corresponding flame heights table
ENTIRELY CONFINED FLOW

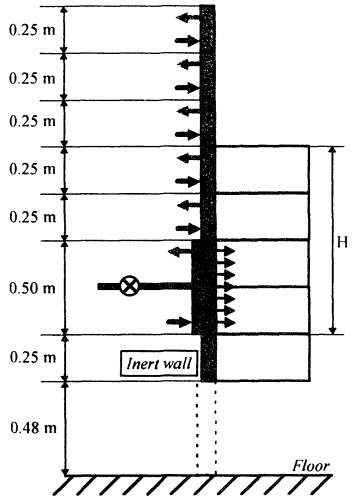

Figure 2a
Burner of 0.50x0.40 m²

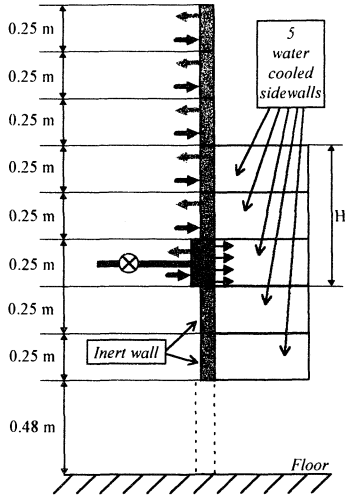

Figure 2b
Burner of 0.25x0.40 m²

	Q_{th} (kW)	L_{int} (m)	L_{bin} (m)	L_{fluc} (m)	L_f (m)
CH_4	**18**	0.692	0.694	0.680	**0.689**
	27	0.840	0.840	0.844	**0.841**
	36	1.126	1.130	1.124	**1.127**
	45	1.287	1.287	1.292	**1.289**
	54	1.402	1.393	1.413	**1.403**
	63	1.458	1.464	1.470	**1.464**
	72	1.574	1.577	1.578	**1.576**
C_3H_8	**18**	0.629	0.628	0.631	**0.629**
	27	0.836	0.833	0.834	**0.834**
	36	1.081	1.080	1.080	**1.080**
	45	1.227	1.229	1.222	**1.226**
	54	1.331	1.326	1.324	**1.327**
	63	1.404	1.399	1.404	**1.402**
	72	1.511	1.504	1.516	**1.510**
C_2H_2	**27**	0.890	0.885	0.893	**0.889**
	36	1.060	1.060	1.065	**1.062**
	45	1.215	1.213	1.209	**1.212**
	54	1.308	1.303	1.306	**1.306**
	63	1.374	1.374	1.372	**1.373**

Table 2a
Burner of 0.50x0.40 m²

	Q_{th} (kW)	L_{int} (m)	L_{bin} (m)	L_{fluc} (m)	L_f (m)
CH_4	**18**	0.775	0.773	0.774	**0.774**
	27	0.975	0.964	0.978	**0.972**
	36	1.167	1.164	1.171	**1.167**
	45	1.292	1.296	1.291	**1.293**
	54	1.421	1.417	1.416	**1.418**
	63	-	-	-	-
	72	-	-	-	-
C_3H_8	**18**	0.746	0.742	0.744	**0.744**
	27	0.914	0.918	0.919	**0.917**
	36	1.078	1.078	1.087	**1.081**
	45	1.232	1.221	1.223	**1.225**
	54	1.314	1.317	1.314	**1.315**
	63	1.414	1.417	1.410	**1.414**
	72	-	-	-	-
C_2H_2	**27**	0.932	0.935	0.943	**0.937**
	36	1.032	1.032	1.039	**1.034**
	45	1.124	1.121	1.121	**1.122**
	54	1.167	1.160	1.174	**1.167**
	63	-	-	-	-

Table 2b
Burner of 0.25x0.40 m²

FIGURE 2 : Experimental setup and corresponding flame heights table
PARTIALLY CONFINED FLOW

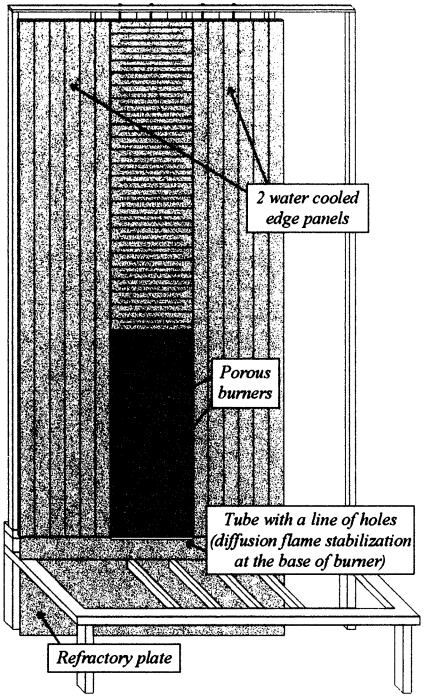

Figure 3a
Burner of 1x0.40 m²

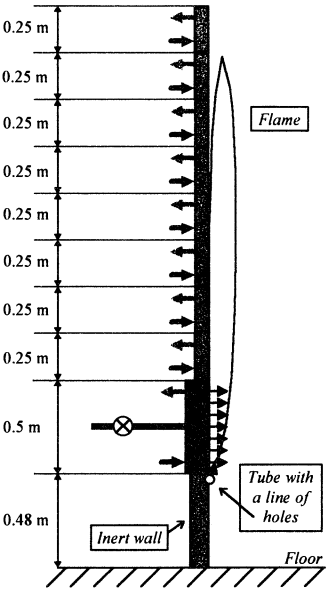

Figure 3b
Burner of 0.50x0.40 m²

	Q_{th} (kW)	L_{int} (m)	L_{bin} (m)	L_{fluc} (m)	L_f (m)
C_3H_8	**27**	-	-	-	-
	36	-	-	-	-
	45	1.143	1.155	-	**1.149**
	54	1.419	1.419	1.434	**1.424**
	63	1.612	1.615	1.602	**1.610**
	72	1.736	1.746	1.739	**1.740**
	81	1.842	1.848	1.851	**1.847**
	90	1.930	1.933	1.917	**1.927**
	99	1.989	1.995	1.996	**1.993**

Table 3a
Burner of 1x0.40 m²

	Q_{th} (kW)	L_{int} (m)	L_{bin} (m)	L_{fluc} (m)	L_f (m)
C_3H_8	**27**	0.983	0.988	0.991	**0.987**
	36	1.183	1.186	1.185	**1.185**
	45	1.338	1.345	1.338	**1.340**
	54	1.524	1.533	1.546	**1.534**
	63	1.622	1.643	1.677	**1.647**
	72	1.779	1.786	1.804	**1.790**
	81	1.893	1.902	1.914	**1.903**
	90	1.938	1.941	1.963	**1.947**
	99	2.000	2.020	2.010	**2.010**

Table 3b
Burner of 0.50x0.40 m²

FIGURE 3 : Experimental setup and corresponding flame heights table
UNCONFINED FLOW